http://dx.doi.org/10.1590/1678-4162-11987

C.R. Andrade
https://orcid.org/0000-0003-0761-6652
B.W. Minto
https://orcid.org/0000-0002-8808-4127
R.M. Dreibi
https://orcid.org/0000-0002-7705-6075
L.M.I. Diogo
https://orcid.org/0000-0003-2545-8299
T.A.S.S. Rocha
https://orcid.org/0000-0003-1414-3101
F.Y.K. Kawamoto
https://orcid.org/0000-0002-9569-6455
G.G. Franco
https://orcid.org/0000-0001-9945-3453
R.A.R. Uscategui
https://orcid.org/0000-0002-9760-8631
L.G.G.G. Dias
https://orcid.org/0000-0003-3993-1649

***Arq. Bras. Med. Vet. Zootec.*, v.73, n.3, p.571-582, 2021**

Comparison of radiographic and tomographic evaluations for measurement of the Canal Flare Index in dogs

[*Comparação entre avaliação radiográfica e tomográfica para mensuração do Canal Flare Index em cães*]

C.R. *Andrade*[1], B.W. *Minto*[1], R.M. *Dreibi*[1], L.M.I. *Diogo*[1], T.A.S.S. *Rocha*[2], F.Y.K. *Kawamoto*[3], G.G. *Franco*[4], R.A.R. *Uscategui*[5], L.G.G.G. *Dias*[1]

[1]Faculdade de Ciências Agrárias e Veterinárias - Universidade Estadual Paulista - Jaboticabal, SP
[2]Universidade Brasil – Descalvado, SP
[3]Centro Universitário de Lavras - Lavras, MG
[4]Universidade Federal do Espírito Santo - Alegre, ES
[5]Instituto de Ciências Agrárias - Universidade Federal dos Vales do Jequitinhonha e Mucuri - Unaí, MG

ABSTRACT

The outcome of total hip arthroplasty (THA) in dogs is directly related to surgical planning. Templating of radiographs prior to THA should help the surgeon anticipate prosthesis size and femoral shape allowing canal fill of the proximal metaphysis by the implant ensuring primary stable fixation. The canal flare index (CFI) obtained from radiograph has been used as a measure of risk of complications for the technique in human beings and dogs. However, standard radiographs only provide limited data for the selection of cementless prostheses and the assessment of their fit within the femoral canal, due to factors like radiographic magnification and femoral rotation. Therefore, three-dimensional evaluation based on computed tomography (CT) may be a better tool for CFI measurement. The aim of this study was to compare anatomical measurement with CFI values obtained from craniocaudal radiography and CT. Craniocaudal radiographs using a horizontal radiographic beam (CR), CT, and anatomical macroscopic measurements (A) were obtained from 45 femurs from 23 canine cadavers. The differences between the values of CFI obtained from radiograph (CFI-R), computed tomography on transverse (CFI- TT) and longitudinal axis (CFI-TL) compared to the CFI obtained from macroscopic measurements - gold standard - (CFI-A), and 95% limits of agreement (LOA) between the values, were evaluated by the Bland-Altman method. Dimensions obtained from CT techniques had a greatest mean difference from anatomical and CFI values were also different (P=0.032). Under the experimental conditions, the craniocaudal radiograph, provided the most accurate measurement of the CFI (mean difference: 0.087 ± 0.42).

Keywords: computed tomography, craniocaudal projection, cementless THR, femoral morphology, three-dimensional analysis

RESUMO

O resultado da artroplastia total do quadril (ATQ) em cães está diretamente relacionado ao planejamento cirúrgico. O templating *radiográfico pré-operatório da ATQ deve ajudar o cirurgião a prever o tamanho da prótese e o formato do fêmur, o que permitirá um preenchimento ideal da metáfise proximal pelo implante, garantindo, assim, fixação primária estável. O índice de alargamento do canal (*Canal Flare Index - *CFI) obtido em radiografias tem sido utilizado como fator de risco de complicações para a técnica em humanos e cães. No entanto, as radiografias podem fornecer apenas dados limitados para a seleção de próteses não cimentadas e a avaliação do seu encaixe no canal femoral, devido a fatores como ampliação radiográfica e rotação femoral. Portanto, a avaliação tridimensional baseada na tomografia computadorizada (TC) pode ser uma ferramenta vantajosa para a mensuração do CFI. O objetivo deste estudo foi comparar a medida anatômica com os valores de CFI obtidos na radiografia craniocaudal e na*

Recebido em 15 de abril de 2020
Aceito em 14 de dezembro de 2020
E-mail: carolrdeandrade@hotmail.com

TC. Radiografias craniocaudais utilizando feixe radiográfico horizontal (CR), tomografia computadorizada e medidas macroscópicas anatômicas (A) foram obtidas de 45 fêmures de 23 cadáveres caninos. As diferenças entre os valores de CFI obtidos na radiografia (CFI-R), na tomografia computadorizada no eixo transversal (CFI-TT) e no eixo longitudinal (CFI-TL), em comparação com os valores de CFI obtidos nas medições macroscópicas – padrão-ouro – (CFI-A) e os limites de concordância de 95% (LOA) entre os valores, foram avaliadas pelo método de Bland-Altman. As dimensões obtidas pelas técnicas de TC apresentaram maior diferença média dos valores anatômicos, e as do CFI também foram diferentes (P=0,032). Nas condições experimentais, a radiografia craniocaudal forneceu a medida mais precisa do CFI (diferença média: 0,087 ± 0,42) para representar o padrão-ouro deste estudo.

Palavras-chave: tomografia computadorizada, projeção craniocaudal, morfologia femoral, análise tridimensional, substituição total de quadril não cimentada

INTRODUCTION

Variations in proximal femoral morphology, especially those associated with total hip arthroplasty (THA), have been studied by orthopedic surgeons for at least three decades (Noble *et al*., 1988; Rashmir-Raven *et al*., 1992; Husmann *et al*., 1997; Palierne *et al*., 2006; Pugliese, 2014; Tawada *et al*., 2015; Sevil-Kilimci and Kara, 2016). The radiographic evaluation of the proximal femoral medullary canal, provides standardized femoral measurements, including the canal flare index (CFI) (Rubin *et al*., 1992; Palierne *et al*., 2006). CFI characterizes the ratio between the diameter of the proximal femoral canal and the isthmus. Initially defined in human beings (Noble *et al*., 1988; Husmann *et al*., 1997), CFI values were later established in dogs (Rashmir-Raven *et al*., 1992; Palierne *et al*., 2006, 2008) allowing the classification of the femurs into three categories: stovipipe shape, normal shape and champagne-flute shape. Since then, CFI has been widely used for femoral stem selection in THA planning in both human and veterinary medicine.

The preoperative calculation of CFI to determine the potential for subsidence is an important key in the evaluation of such dogs as candidates for cementless THA (Rashmir-Raven *et al*., 1992; Liska and Doyle, 2015) because femoral morphology and percentage of canal fill by the prosthetic stem are predictors of subsidence (Liska and Doyle, 2015). Additionally, association between CFI and subsidence of the stem and femoral fractures after uncemented THA in dogs has been reported (Rashmir-Raven *et al*., 1992; Ganz *et al*., 2010). Dogs with a stovepipe-shaped account for a significant percentage of dogs that undergo THA, resulting in cemented stems being used more frequently in the past (Rashmir-Raven *et al*., 1992).

Today, a collared stem designed to resist subsidence and assist in stabilizing the stem for bone in growth in the early post-op period, especially for large breed dogs and dogs with a low canal flare index is available (Liska and Doyle, 2015). Thus, making the correct decision when selecting design and implant size could be directly related with a precise CFI calculation on preoperative templating. However, the variations on proximal femur endosteal width may not be visible on conventional radiographs due to the two-dimensional image limitations to represent femoral canal (Rubin *et al*., 1992; Tawada *et al*., 2015), mainly caused by femoral rotation and directly affecting CFI (Andrade *et al*., 2019). Eckrich *et al*. showed that only 10º of internal femoral rotation caused a reduction in proximal canal width of 0.9 ± 0.4mm.

CT provides a three-dimensional evaluation of tissue structures and has been studied in the context of modeling and measurement of bone geometry for THA (Pugliese, 2014). In man, the *in vitro* comparison of radiographic and tomographic measurements with the true anatomical dimensions showed that CT provided greater precision for assessment of femoral geometry (Rubin *et al*., 1992). However, similar studies have not yet been performed in dogs. Morphological studies using CT and three-dimensional image reconstruction for the validation of the radiographic estimation of CFI has potential for the standardization of this technique in dogs (Tawada *et al*., 2015). The aim of this study was to compare the values of CFI obtained from craniocaudal radiography using a horizontal radiographic beam technique and computed tomography (CT), with values obtained from the direct measurement of anatomical specimens.

MATERIAL AND METHODS

The study was approved by the Ethics Committee on the Use of Animals (CEUA) of the of the Faculty of Agrarian and Veterinary Sciences, São Paulo State University, Jaboticabal, São Paulo, Brazil (protocol nº 004505/17). Skeletally mature canine cadavers of different breeds were used. Animals had died or were euthanized in the Clinical and Surgical Service of the Veterinary Hospital "Governador Laudo Natel" for reasons not related to the study. The inclusion criteria were skeletally mature dogs weighing >20kg, without apparent signs of bone neoplasia and fractures. The right and left femurs were considered as separate units, providing a total sample size of 46 femurs. All cadavers were radiographed followed by anatomical dissection of femora, CT and anatomical macroscopic measurements (A) of specimens.

The CFI was calculated by three evaluators (LGGGD; FKK; GGF – all experienced surgeons) using three different techniques: craniocaudal radiograph using a horizontal radiograph beam (R), computed tomography (CT) and anatomical macroscopic measurements (A). The cadavers were radiographed using digital radiographic equipment (radiographic equipment, Siemens® RG150 / 100gl, Siemens, Germany) using 66 Kvp, 200 mA, 5 mAs, CR30 -X digitizer (CR30-X digitizer, Agfa Healthcare, Brazil) and a CR MD4.0T 43x35 cassette (CR MD4.0T cassette, Agfa Healthcare, Brazil). For the radiographical study, the pelvic limbs were clipped to facilitate visual positioning of the femurs and the placement of the magnification indicator.

The magnification indicator was attached to the skin surface, parallel to each femur in the region of the greater trochanter in all radiographs. The x-ray beam was positioned perpendicular to the examination table, the cadaver positioned in lateral recumbency, with the pelvic limbs parallel to the x-ray source. The uppermost limb positioned in hyperextension, in a neutral axis of rotation, with the patella centered between the condyles and directed to the x-ray source. The cassette was placed immediately caudal to, and parallel with, the femur. For inclusion the images had to show parallel femurs, the patella centered on the trochlear sulcus and fabella bisected by the femoral cortex, vertical walls of the intercondylar notch are distinct parallel lines, and the lesser trochanter partially visible. The digital radiographic images of each femur that met the inclusion criteria were stored in software for visualization and manipulation of digital medical images (EPACS WORKSTATION 5.0 software measurement, EPACS WORKSTATION®, Brazil).

They were analyzed individually and read independently by the evaluators who each calculated the CFI values. For the CFI calculation from radiographic measurements, a software measurement tool (EPACS WORKSTATION 5.0 software measurement, EPACS WORKSTATION®, Brazil) was used, according to the guidelines previously described (Noble *et al*., 1988; Palierne *et al*., 2006, 2008; Rashmir-Raven *et al*., 1992). The evaluators measured the endosteal width at the level of the midpoint of the lesser trochanter (A) and the endosteal width at the level of the isthmus (B), defined as the diaphyseal region with the narrowest medullary canal (Palierne *et al*., 2008) chosen subjectively by each evaluator. The ratio between endosteal width at the midpoint of the lesser trochanter and endosteal width of the isthmus $\left({}^{A}/_{B}\right)$ determined on the radiograph was denominated CFI-R. Immediately after obtaining the radiographic images, the femurs were dissected and stored at - 20°C, until computed tomography and anatomical measurements were performed.

For CT, all the specimens (femur previously dissected) were positioned with the trochlear surface facing up, supported on the condyles, keeping the parallelism of the bone relative to table. Using helical CT and only selecting the femora in the field of view (FOV), the specimens was examined at 1.25mm thickness intervals and 2.5mm sections using tomographic equipment (GE LightSpeed ™ RT16/Xtra tomographic equipment, General Electric®, USA) and the CT data were digitally transferred from the scanner console to the planning workstation using a DICOM interface (Digital Imaging and Communications in Medicine). The morphometric measurements were performed with three-dimensional reconstruction software for medical images (Radiant DICOM Viewer 4.0

software for medical images, Radiant®, Poland), and the reference points and measurements were adapted from previous studies (Noble *et al*., 1988; Palierne *et al*., 2006, 2008; Rashmir-Raven *et al*., 1992).

Using the 3D reconstruction measurement tool, the femoral length was measured and the distance from the midpoint of the lesser trochanter to the proximal end of the greater trochanter was measured (Figure 1 - A). To make sure that the endosteal width at the two points used for CFI calculation (lesser trochanter and isthmus) was measured in the central section of the femur both longitudinally and transversely, the 3D multiplanar reconstruction (MPR 3D) of the software (Radiant DICOM Viewer 4.0 software for medical images, Radiant®, Poland) was used. In addition, certain guidelines were set for all the evaluators: the proximal half of the femur was divided into 3 parts in the sagittal plane.

The extracortical width was measured at the 3 points where the femur was sectioned and the y-axis of the 3D MPR was positioned at the midpoint of each of the three measurements (Figure 1 - B). As in the radiographic evaluation, the evaluators measured the endosteal width in both dorsal and transverse planes at the level of the midpoint of the lesser trochanter and at the level of the isthmus, which was subjectively determined by each evaluator on the longitudinal section of the femur in transverse plane (Figure 2). The ratio between the endosteal width at the level of the lesser trochanter and the endosteal width of the isthmus $\left(A/_B\right)$ determined on the two CT sections were denominated the longitudinal tomographic CFI (CFI-TL) and transverse tomographic CFI (CFI-TT).

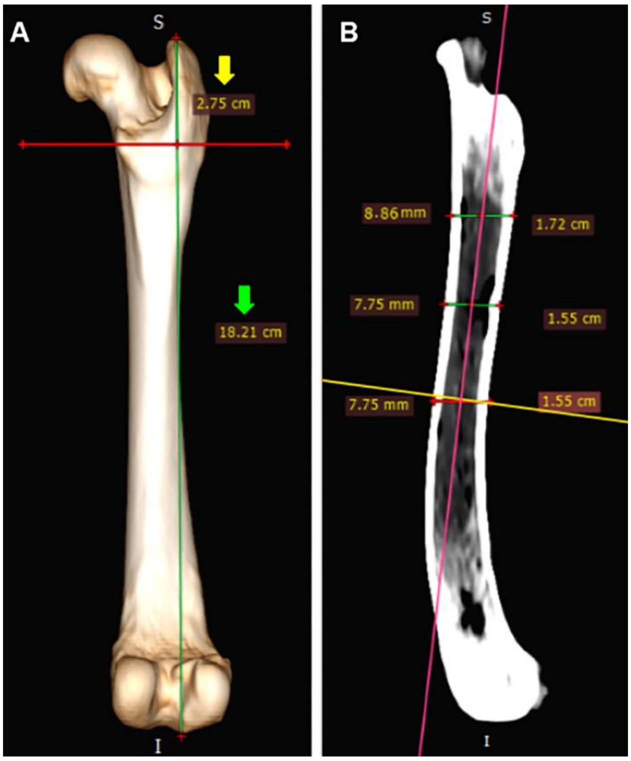

Figure 1. Tomographic image of the right femur of a dog. (A) 3D reconstruction (caudal view), showing measurement of total femur length (green arrow), from the proximal end of the greater trochanter to the horizontal plane tangential to the femoral condyles, and location of the midpoint of the lesser trochanter (yellow arrow). (B) 3D multiplanar reconstruction (medial view), with proximal femoral divisions and midpoint location in each portion. Pink: y-axis; yellow line (x-axis); measures of extracortical width: right side of figure; mid-point measurements: left side of figure.

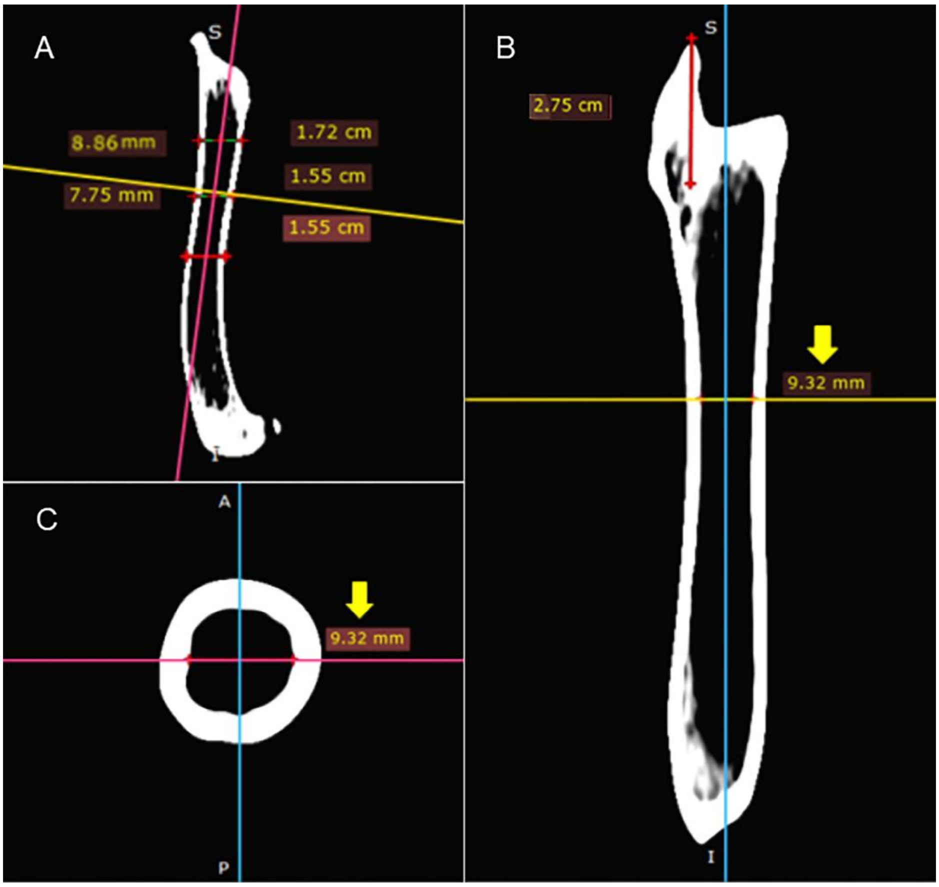

Figure 2. Tomographic image of right canine femur in multiplanar 3D reconstruction. (A) Medial view of the femur with the y-axis (pink line) positioned centrally within the femur and the x-axis (yellow line) positioned on the isthmus. (B) Measurement of the intracortical width of the isthmus (yellow arrow) in the longitudinal section of the femur; red line: level of the midpoint of the lesser trochanter. (C) Measurement of the intracortical width of the isthmus (yellow arrow) in the cross section of the femur.

In the previously dissected femur, the total femoral length was measured in mm, from the proximal border, delimited by the tangent line to the greater trochanter, to the distal border, represented by the tangent line to the condyles. A mark was made at the halfway point and cuts were made using an electric band saw (electric band saw, Starret®, USA). The femur was initially divided transversely and parallel to the bicondylar plane at two points (halfway along the femoral length and at the midpoint of the lesser trochanter) giving rise to three fragments: proximal, intermediate and distal (Figure 3 - A). Then, the midpoint of the intermediate fragment was identified in the mediolateral plane using a digital caliper (digital caliper 300mm, Mitutoyo®, Brazil) and a longitudinal section was created (Figure 3 – B), giving rise to two new fragments, cranial and caudal (Figure 3 – C). The caudal fragment was used for anatomical measurement of the CFI. Using a digital caliper (digital caliper 300mm, Mitutoyo®, Brazil), the evaluators measured the endosteal width on the proximal face of the caudal intermediate fragment (midpoint of the lesser trochanter) and the endosteal width at the level of the isthmus, following the guidelines used in the radiographic measurement. The ratio obtained was denominated anatomical CFI (CFI-A).

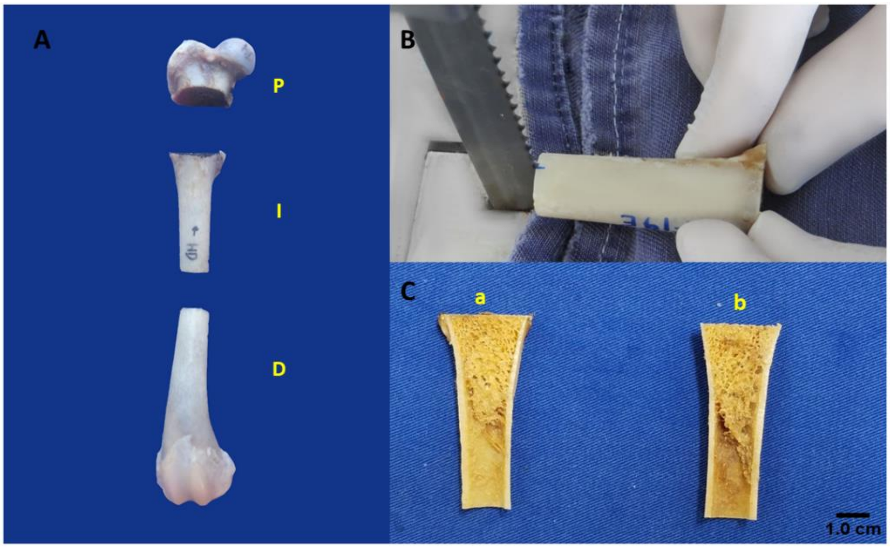

Figure 3. (A) Photographic image of a right canine femur after anatomical dissection and section at the two points (midpoint of the lesser trochanter and isthmus), producing three fragments: proximal (P), intermediate (I) and distal (D). (B) Photographic image of the longitudinal sectioning of the intermediate fragment using band saw. (C) Longitudinal section of the intermediate femoral fragment, giving rise to two new cranial (b) and caudal (a) fragments, where (a) is used for direct measurement of the CFI.

The statistical analyses were performed using a statistical package program (R statistical package program, R Foundation for Statistical Computing, Austria). Using the software, the resulting values were initially tested for the homoscedasticity of variances (Bartlett test) and the normal distribution of residues (Shapiro-wilk test). The calculated measures of the CFI (CFI-R, CFI-TL, CFI-TT and CFI-A) were compared among the evaluators by analysis of variance (ANOVA) and the means compared by the Tukey test. Later, the calculated measurements of the radiographic (CFI-R;) and tomographic CFI (CFI-TL, CFI-TT) were compared to the CFI-A by ANOVA and, if significant, the means compared by the Bonferroni test. Significance was set for all tests at 95% ($p \leq 0.05$) and data presented as the mean ± standard deviation (SD). The limits of agreement (LOA) between the CFI values obtained by the anatomical measurement (CFI-A), craniocaudal horizontal beam radiography (CFI-R) and computed tomography (CFI-TL, CFI-TT) were evaluated by the Bland-Altman method (Bland and Altman, 2007).

RESULTS

Twenty-three cadavers meet the inclusion criteria, 8 males and 15 females, with a mean weight of 23.8 ± 4.5kg. The final sample size was 45 femurs, due to the fracture of a tibia during radiographic positioning, which probably occurred because the cadaver was still partly frozen at the time of radiographic positioning. Therefore, the correct positioning of the limb for radiography was impaired, excluding this femur from the study. The sample size used in this study made it possible to achieve a statistical power of 70% (1-β) in the comparative analysis of the CFI between the techniques, using an α 0.05 with an effect f of 0.22, this calculation was performed using the G* Power® software (Version 3.1.9.2, Universität Kiel, Germany).

There was no difference between examiners except for the tomography cross-section measurement (CFI-TT) (P=0.0371), the mean and the standard deviation of the other techniques are shown in Table 1. The mean and standard deviation of the endosteal width at the level of the lesser trochanter and isthmus of the 45 femurs, obtained in the four techniques compared, are shown in Table 2. Table 3 show the results referring to the values obtained by each of the techniques used to calculate CFI and their respective comparisons. The correlation between radiographic and tomographic techniques with the data obtained from the macroscopic evaluation, reveals a poor intraclass correlation index (ICC) and confidence interval (Table 3). Concordance of the measurements is shown in Figure 4, the mean difference using Bland-Altman analysis was lower when the anatomical measurement (CFI-A) was compared to the craniocaudal radiograph (CFI-R) (Figure 4-B) rather than the two tomographic techniques (CFI-TT, CFI-TL) (Figure 4-B and C). In addition, when CFI-A was compared to the CFI obtained in the three measurement techniques (CFI-R, CFI-TT and CFI-TL), the only difference was for CFI-TL (P=0.032) (Figure 4-A).

Table 1. Evaluation of the interobserver difference. Canal Flare Index (CFI) value (mean ± SD) of the evaluators, and p value according to the technique used

Technique	Evaluator	CFI	p-evaluator
Craniocaudal radiograph	1	2.04±0.27	0.0739
	2	2.03±0.27	
	3	1.94±0.31	
Longitudinal tomography section	1	2.04±0.37	0.1762
	2	1.97±0.35	
	3	1.90±0.34	
Transverse tomography section	1	2.07±0.34	0.0371*
	2	1.95±0.19	
	3	1.90±0.30	
Anatomical preparation	1	2.05±0.38	0.1016
	2	2.19±0.46	
	3	2.03± 0.38	

CFI – canal flare index

Table 2. Descriptive statistics of the measurements obtained in the two anatomical regions (lesser trochanter and isthmus) of 45 canine femurs, used to calculate the Canal Flare Index in the four evaluation techniques used

Dimension (cm)	Technique			
	A[a]	R[b]	TL[c]	TT[d]
	Mean SD	Mean SD	Mean SD	Mean SD
Canal width (lesser trochanter)	2.034 ± 0.254	2.098 ± 0.232	1.898 ± 0.303	1.922 ± 0.264
Canal width (isthmus)	0.997 ± 0.160	1.064 ± 0.155	0.981 ± 0.147	0.988 ± 0.146

[a] Anatomical preparation
[b] Craniocaudal radiograph
[c] Longitudinal tomography section
[d] Transverse tomography section

Table 3. Descriptive statistics of the Canal Flare Index (CFI) measurements obtained in four evaluation techniques (anatomical preparation, craniocaudal radiography with horizontal beam, computed tomography – longitudinal and transverse section) in canine femurs (n = 45)

	CFI			
	A	R	TL	TT
Mean ± SD	2.090 ± 0.039	2.003 ± 0.039	1.968± 0.042	1.976 ± 0.042
Mean Diff. (bias) ± SD		0.087±0.421	0.122 ±0.398	0.114±0.395
95% B-A Limits of agreement		-0.737 to 0.912	-0.658 to 0.902	-0.660 to 0.889
p-Value *vs.* A		0.443	0.061	0.032*
Intraclass Correlation Coefficient		0.362	0.486	0.347
ICC 95%-Confidence Interval		0.21 to 0.50	0.35 to 0.61	0.19 to 0.49

A- Anatomical preparation
R- Craniocaudal radiograph
TL- Longitudinal tomography section
TT- Transverse tomography section
Bias- Difference between the two CFI measures when compared to the anatomical one
B-A: Bland-Altman 95% LOA

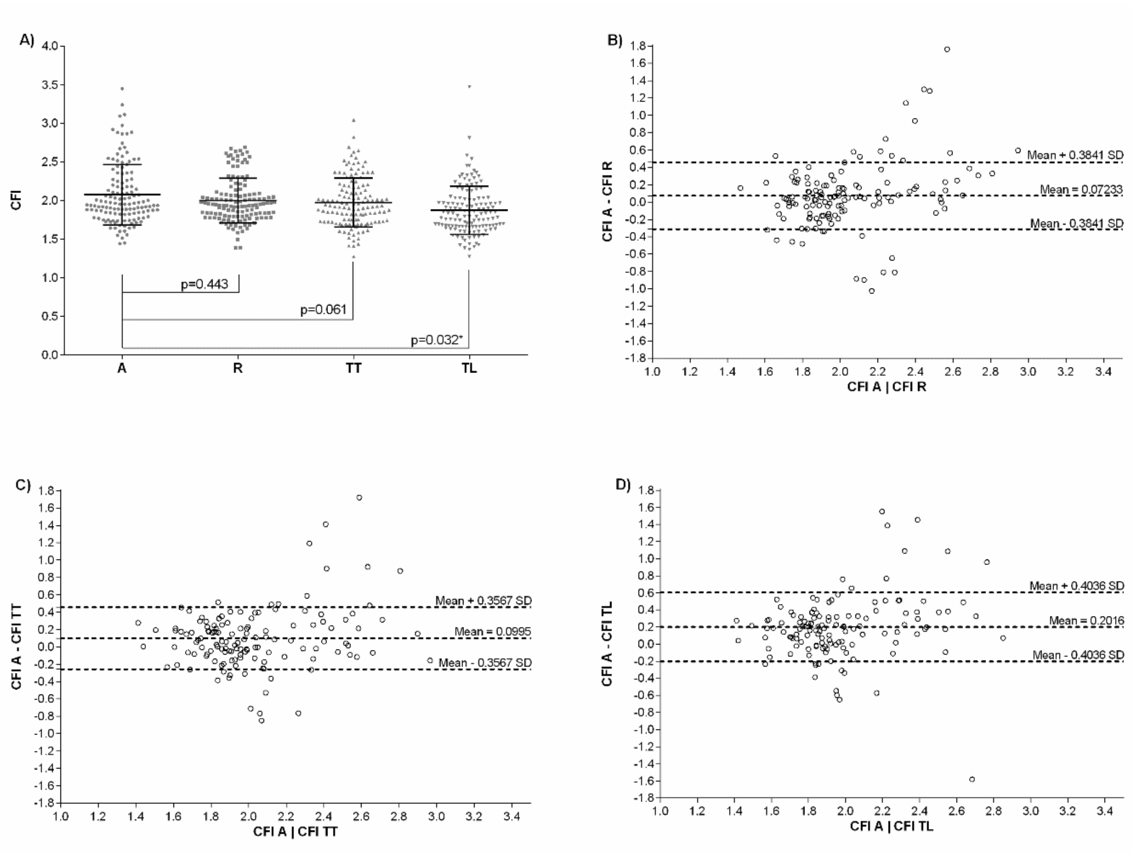

Figure 4. (A) Distribution, mean and standard deviation of the Canal Flare Index (CFI) in canine femurs according to the evaluation method used: (A) anatomical macroscopic measurements, (R) craniocaudal radiograph with horizontal beam, transverse tomography section (TT) and longitudinal tomography section (TL). (B, C and D) Bland-Altman plots illustrating agreement between CFI as measured by anatomical macroscopic compared to radiography (B) and CT (C and D). Values given in centimeters with mean difference (mean) and LOA (mean ± SD). The dashed lines represent the limits of agreement.

DISCUSSION

Although conventional radiographs of the locomotor system are still widely used there is increasing interest in three-dimensional examination of these structures (Railhac *et al*., 1997). Under experimental conditions, CT was describe as better for morphometric analysis of the proximal femur than standard radiographs, which provided insufficiently accurate radiographic measurements for preoperative planning of THA and custom-made prosthesis manufacturing (Rubin *et al*., 1992). According to Husmann *et al*. (1997) CT is currently the best technique for an anatomical study in clinical practice using uncemented femoral prostheses. However, in our study, craniocaudal radiography was superior to the CT technique.

The mean difference (bias) of the CFI measurement in tomography in both longitudinal and transverse sections was higher than that found for radiography, showing greater concordance of radiographic measurements when compared to anatomical evaluation. In addition, the CFI values in the longitudinal tomographic measurement (CFI-TL) were different (P=0.032) from the CFI-A, and CFI-R was the most similar (P=0.443). The data spread (SD) of CT measurements is higher than radiographic measurements suggests that there were inconsistencies in CT measurements. We believe that this observation is partially related to the reduced familiarity of the evaluators with the measurement using CT comparatively to radiography. Although in a study using radiography for digital pre-operative templating of THA, the experience of the planner does not significantly affect the accuracy of correctly predicting component sizes (Shichman *et al*., 2020).

In man, several three-dimensional studies of femoral morphology using CT have been performed, all of which showed it to be superior to radiography in the morphometric representation of the proximal femur and in the planning of the THA (Rubin *et al*., 1992; Viceconti *et al*., 2003). Similarly, superiority of CT has been reported for humerus CFI evaluation in dogs, Smith *et al*. (2017) have observed that radiographic craniocaudal CFI measurements were 13% less than CFI measurements on CT images. However, the difference could have been the result of a disparity between the dogs evaluated radiographically and by use of CT, that were not the same. Studies using CT to asses femoral canal have been reported (Pugliese, 2014; Sevil-Kilimci and Kara, 2016, 2020), but neither compared radiographic and tomographic data with true anatomical dimensions.

Studies in people and dogs that showed CT superiority used software with semi-automatic or even automatic selection of the femoral endosteal limits (Rubin *et al*., 1992; Tawada *et al*., 2015; Sevil-Kilimci and Kara, 2016, 2020). In a study developed by Sevil-Kilimci *et al*. (2016) the images were processed using software to obtain 3D reconstructions of the internal and external geometries of each femur with semi-automatic segmentation of the cortical bone limits. In addition, the digital radiographic images were used to define the bone boundaries. Aiming a clinical scenario in which a surgeon manually draws lines using standard picture archiving and communications system tools, the present study used basic three-dimensional medical image reconstruction software, which did not allow automatic delimitation between cortical bone and the medullary canal.

Thus, the measurements were manually delimited by the evaluators, which may have significantly increased the error rate. However, the studies in people and dogs that showed CT superiority used software with semi-automatic or even automatic selection of the femoral endosteal limits (Rubin *et al*., 1992; Tawada *et al*., 2015; Sevil-Kilimci and Kara, 2016). In a study developed by Sevil-Kilimci *et al*. (2016) the images were processed using software to obtain 3D reconstructions of the internal and external geometries of each femur with semi-automatic segmentation of the cortical bone limits. In addition, the digital radiographic images were used to define the bone boundaries (Sevil-Kilimci and Kara, 2016). Another finding that demonstrated the decreased accuracy of tomographic data is the variation between the evaluators for measurements in the same femur (P=0.0371) in the tomography cross section (CFI-TT).

There was inevitably evaluator variation in defining different endosteal limits caused by study methodology. An excellent intraobserver and interobserver reliability reflects, at least in part, the use of a customized programming model to reduce error (Boissonneault *et al*., 2017). In the current study a poor intraclass correlation index (ICC) and confidence interval was observed between radiographic and tomographic techniques with the data obtained from the macroscopic evaluation. However, radiographic measurement showed better agreement with the anatomic one, and the bias between methods was the lowest. Usually, the interobserver agreement is lower than the intraobserver agreement for the estimate of the same sample, because it incorporates variability inherent to different evaluators. In addition, the ICC estimate for single measures generates smaller estimates than the estimate for average measures, which justifies the use of multiple measures to reduce random error (Amante, 2016), which was not realized in the present study.

The mean endosteal width of the two regions studied (lesser trochanter and isthmus), obtained through cross-sectional or longitudinal tomography, differed from that reported by Sevil-Kilimci *et al*. in two different breeds. Consequently, the mean CFI for the population was also different (Sevil-Kilimci and Kara, 2016). However, the methodology used may have influenced the values, because that study used only German Shepherd and Kangal breed dogs, with a mean weight of 28.81 ± 7.33 and 41.75 ± 9.90, respectively, that differed from our study. In addition, Sevil-Kilimci *et al*. used the endosteal width of the proximal end of the lesser trochanter for CFI calculation.

The data spread of anatomic measurements higher than radiographic measurements observed is an important finding that suggests inconsistencies in anatomic measurement methods. The use of anatomic macroscopic measurement as a gold standard were reported in humans (Sen *et al*., 2010) and dogs (Andrade *et al*., 2019). However, the femoral canal has a variability of the normal cross-sectional shape of the medullary canal at different levels, which is somewhat pear shaped proximally, assuming a funnel shape in diaphyseal area (Eckrich *et al*., 1994; Sen *et al*., 2010), thus cutting the bone based on midpoint the mediolateral plane of the diaphysis or off center may have resulted in an underestimated value. Furthermore, there are significant differences in the size of the endosteal canal and in the relative amount of trabecular bone between normal and stovepipe femora (Pugliese, 2014), which was probably affected by use of thawed cadavers using in the study.

It is known that correct radiographic positioning of the patient may be difficult because of pain or contracture, and small variations in leg rotation significantly alter some of the dimensions, such as neck-shaft angle, calcar curvature, and isthmus width (Rubin *et al*., 1992; Casper *et al*., 2012). Similarly, the use of cadavers in our study to mimic the clinical situation may have resulted in the same effect. However, Andrade *et al*. (2019) showed that the craniocaudal projection with a horizontal radiographical beam is the radiographic technique that provides the best approximation of the true anatomical dimensions of the canine femur, reducing the influence of the technique on the CFI values.

Although the average difference (Bias) in the radiographic and tomographic techniques (CFI-H, CFI-TL, CFI-TT) when compared to the anatomical measurement (CFI-A) was close to zero, individual differences could be so great as to change the category of femur and may be clinically significant. Although the horizontal beam radiographic technique also causes this effect, changes are less likely. When these differences are brought into practice, patients with CFI near the limits of the category may change classification category. If we consider a cementless off-the-shelf prostheses on the market, like Universal Hip System BFX (BioMedtrix, New Jersey, USA), and look at the range of frontal widths at the proximal level, we find, for the five sizes of stem, that the variation between one size and the next is from 0.8 to 2.0 mm. Our results show that the standard deviation in measuring the proximal region using tomographic longitudinal or transverse analysis is greater (3.03 mm and 2.62 mm, respectively) than radiographic analysis (2.32 mm). Consequently, the biggest impair in stem selection is using the tomographic technique.

In view of the limitations of the technique for tomographic measurement of CFI, the authors believe that CT is undoubtedly a tool that will bring advances to surgical planning and in the development of custom-made prostheses for dogs, but suggest that previously developed standards for CFI (based on standard radiographs using measurements in the coronal plane) (Rashmir-Raven *et al*., 1992) may not be appropriate. In a study by Pugliese (2014), evaluating the proximal femur morphology and bone quality in dogs using CT, dogs with lower CFI had a smaller fraction of trabecular bone within the endosteal cavity than dogs with greater CFI, suggesting that CFI may be useful in the prediction of bone microstructure. This finding could explain the fact that stovepipe femurs are more predisposed to stem subsidence and femoral fracture. However, these results were obtained through the volumetric calculation of the proximal femur region, and not through two-dimensional CT measurements.

The use of a widely used and simple image reconstruction software that mimics under the more likely clinical scenario in which a surgeon manually draws lines using standard PACS tools like in the current study is not applicable. We believe that the calculation of CFI using CT in dogs requires a methodology different from that already established in dogs using radiography and future studies should investigate the use of an image processing software for 3D design and modeling that demarcate boundary regions between the cortical bone and the cancellous bone.

CONCLUSIONS

The values of CFI obtained from CT were different from those obtained from the direct measurement of the anatomical specimens. In the current study, only the craniocaudal radiograph using a horizontal beam represented the true anatomical morphology. However, this finding may be due to the lack of precision of the tomographic measurement protocol.

REFERENCES

AMANTE H.M. Análise de concordância em estudos clínicos e experimentais. *J. Vasc. Bras.*, v.15, p.89-92, 2016.

ANDRADE, C.R.; MINTO, B.W.; DREIBI, R.M. Accuracy in determining canal flare index using different radiographical positions for imaging canine femurs. *Vet. Comp. Orthop. Traumatol*., v.32, p.234-240, 2019.

BLAND, J.M.; ALTMAN, D.G. Agreement between methods of measurement with multiple observations per individual. *J. Biopharm Stat.*, v.17, p.571-582, 2007.

BOISSONNEAULT, A.R.; HIRANAKA, T.; ROBERSON, J.R.; BRADBURY, T.L. A validated single-view radiographic alternative to computed tomography for the measurement of femoral anteversion: a method-comparison study. *J. Arthroplasty*, v.32, p.1018-1023, 2017.

CASPER, D.S.; KIM, G.K.; PARVIZI, J.; FREEMAN, T.A. Morphology of the proximal femur differs widely with age and sex: relevance to design and selection of femoral prostheses. *J. Orthop. Res.*, v.30, p.1162-1166, 2012.

ECKRICH, S.G.; NOBLE, P.C.; TULLOS, H.S. Effect of rotation on the radiographic appearance of the femoral canal. *J. Arthroplasty*, v.9, p.419-426, 1994.

GANZ, S.M.; JACKSON, J.; VANENKEVORT, B. Risk factors for femoral fracture after canine press-fit cementless total hip arthroplasty. *Vet. Surg.*, v.39, p.688-695, 2010.

HUSMANN, O.; RUBIN, P.J.; LEYVRAZ, P.F. *et al*. Three-dimensional morphology of the proximal femur. *J. Arthroplasty*, v.12, p.444-450, 1997.

LISKA, W.D.; DOYLE, N.D. Use of an Electron beam melting manufactured titanium collared cementless femoral stem to resist subsidence after canine total hip replacement. *Vet. Surg.*, v.44, p.883-894, 2015.

NOBLE, P.C.; ALEXANDER, J.W.; LINDAHL, L.J. *et al*. The anatomic basis of femoral component design. *Clin. Orthop. Relat. Res.*, v.235, p.148-165, 1988.

PALIERNE, S.; ASIMUS, E.; MATHON, D. *et al*. Geometric analysis of the proximal femur in a diverse sample of dogs. *Res. Vet. Sci.*, v.80, p.243-252, 2006.

PALIERNE, S.; MATHON, D.; ASIMUS, E. *et al*. Segmentation of the canine population in different femoral morphological groups. *Res. Vet. Sci.*, v.85, p.407-417, 2008.

PUGLIESE, L. *Proximal femoral morphology and bone quality assessment in dogs.* 2014. 132f. Thesis (Master of Science) - Graduate School of the Ohio State University: the Ohio State University; Columbus.

RAILHAC, J.J.; FOURCADE, D.; HOBATHO, M.C. *et al*. Three-dimensional imaging in orthopaedic surgery: a radiologist's viewpoint. *Injury*, v.28, p.B1-B11, 1997.

RASHMIR-RAVEN, A.M.; DEYOUNG, D.J.; ABRAMS, C.F. *et al*. Subsidence of an uncemented canine femoral stem. *Vet. Surg.*, v.21, p.327-333, 1992.

RUBIN, P.; LEYVRAZ, P.; AUBANIAC, J. *et al*. The morphology of the proximal femur. A three-dimensional radiographic analysis. *J. Bone Joint Surg.*, v.74B, p.28-32, 1992.

SEN, R.K.; TRIPATHY, S.K.; KUMAR, R. *et al*. Proximal femoral medullary canal diameters in Indians: correlation between anatomic, radiographic, and computed tomographic measurements. *J. Orthop. Surg.*, v.18, p.189-194, 2010.

SEVIL-KILIMCI, F.; KARA, M.E. Canal flare index in the canine femur is influenced by the measurement method. *Vet Comp. Orthop. Traumatol.*, v.33, p.198-204, 2020.

SEVIL-KILIMCI, F.; KARA, M.E. The geometry of the proximal femoral medullary canal in German shepherd and kangal dogs. *İstanbul Üniv. Vet. Fak. Derg.*, v.43, p.1-9, 2016.

SHICHMAN, I.; FACTOR, S.; SHAKED, O. *et al.* Effects of surgeon experience and patient characteristics on accuracy of digital pre-operative planning in total hip arthroplasty. *Int. Orthop.*, v.44, p.1951-1956, 2020.

SMITH, E.J.; MARCELLIN-LITTLE, D.J.; HARRYSSON, O.L.A.; GRIFFITH, E.H. Three-dimensional assessment of curvature, torsion, and canal flare index of the humerus of skeletally mature nonchondrodystrophic dogs. *Am. J. Vet. Res.*, v.78, p.1140-1149, 2017.

TAWADA, K.; IGUCHI, H.; TANAKA, N. *et al*. Is the canal flare index a reliable means of estimation of canal shape? Measurement of proximal femoral geometry by use of 3D models of the femur. *J. Orthop. Sci.*, v.20, p.498-506, 2015.

VICECONTI, M.; LATTANZI, R.; ANTONIETTI, B. *et al*. CT-based surgical planning software improves the accuracy of total hip replacement preoperative planning. *Med. Eng. Phys.*, v.25, p.371-377, 2003.